Proton momentum distribution in nuclei beyond ^{4}He

M. K. Gaidarov,[1] A. N. Antonov,[2,*] G. S. Anagnostatos,[2,†] S. E. Massen,[2,‡] M. V. Stoitsov,[1] and P. E. Hodgson[2]
[1]*Institute for Nuclear Research and Nuclear Energy, Bulgarian Academy of Sciences, Sofia 1784, Bulgaria*
[2]*Nuclear Physics Laboratory, Department of Physics, University of Oxford, Oxford OX1-3RH, United Kingdom*
(Received 28 November 1994; revised manuscript received 20 July 1995)

Proton momentum distributions of the ^{12}C, ^{16}O, ^{40}Ca, ^{56}Fe, and ^{208}Pb nuclei are calculated by a model using the natural orbital representation and the experimental data for the momentum distribution of the ^{4}He nucleus. The model allows realistic momentum distributions to be obtained using only hole-state natural orbitals (or mean-field single-particle wave functions as a good approximation to them). To demonstrate the model two different sets of wave functions were employed and the predictions were compared with the available empirical data and other theoretical results.

PACS number(s): 21.60.−n, 21.90.+f

I. INTRODUCTION

The systematic investigations of the nucleon momentum distributions in nuclei extend the scope of the nuclear ground-state theory. Until the mid-1970s more attention in the theory had been paid to the study of quantities such as the binding energy and the nuclear density distribution $\rho(r)$. This is related to the ability of the widely used Hartree-Fock theory to describe these quantities successfully, which, however, are not very sensitive to the dynamical short-range correlations. The experimental situation in recent years concerning the interaction of particles with nuclei at high energies, in particular the $(p,2p)$, $(e,e'p)$, and (e,e') reactions, the nuclear photoeffect, meson absorption by nuclei, inclusive proton production in proton-nucleus collisions, and even some phenomena at low energies such as giant multipole resonances, makes it possible to study additional quantities. One of them is the nucleon momentum distribution $n(k)$ [1,2] which is specifically related to the processes mentioned above. However, it has been shown [3] that, in principle, it is impossible to describe correctly both momentum and density distributions simultaneously in the Hartree-Fock theory. The reason is that the nucleon momentum distribution is sensitive to short-range and tensor nucleon-nucleon correlations. It reflects the peculiarities of the nucleon-nucleon forces at short distances which are not included in the Hartree-Fock theory. This requires a correct simultaneous description of both related distributions $\rho(r)$ and $n(k)$ in the framework of nuclear correlation methods.

The main characteristic feature of the nucleon momentum distribution obtained by various correlation methods [1,2,4–23] is the existence of high-momentum components, for momenta $k>2$ fm^{-1}, due to the presence of short-range and tensor nucleon correlations. This feature of $n(k)$ has been confirmed by the experimental data on inclusive and exclusive electron scattering on nuclei (e.g., [1,2,24–27]). We emphasize also the fact that theoretical results of various correlation methods [9,18,19] as well as experimental data for $n(k)$ obtained by the y-scaling analysis [26] confirm the conclusion [5,28] that the high-momentum behavior of the nucleon momentum distribution [$n(k)/A$ at $k>2$ fm^{-1}] is similar for nuclei with mass number $A=2$, 3, 4, 12, 16, 40, and 56 and for nuclear matter (see [2], p. 139). More precisely, the high-momentum tails of $n(k)$ are almost the same for all nuclei with $A\geq 4$ and thus ^{4}He is the lightest nuclear system that exhibits correlation effects via the high-momentum components of the nucleon momentum distribution. Since the magnitude of the high-momentum tail is proportional to the number of particles, this effect is associated with the nuclear interior rather than with the nuclear surface. This allows us in the present paper to suggest a practical method to calculate the proton momentum distribution for nuclei heavier than ^{4}He (e.g., ^{12}C, ^{16}O, ^{40}Co, ^{56}Fe, and ^{208}Pb) from that of ^{4}He which is already known from the experimental data (or from calculations within correlation methods [2]). Here we should like to emphasize that, though our method has some similarities to the one suggested in [16] (extended and developed in [29–31]), in contrast with the previous calculations, the correlation effects are extracted from ^{4}He rather than from nuclear matter. We should like to mention also that the experimental data for $n(k)$ in ^{4}He (which we use in our calculations) as well as for other nuclei (which we use for a comparison) are not directly measured but are obtained by means of the y-scaling analysis [26] relying on the assumption that the $1/q$ expansion is valid. For this reason we give an additional comparison of the data for $n(k)$ in ^{4}He [26] with the theoretical calculations from [19].

In general, the knowledge of the momentum distribution for any nucleus is important for calculations of cross sections of various kinds of nuclear reactions. It is known that reliable results for $n(k)$ in sophisticated methods such as the exp(S) method [5], the variational method with state-dependent correlations [20], the generator coordinate method (with two generator coordinates [32]), and others are available only for light nuclei up to the ^{16}O nucleus. The local density approximation (LDA) which has been applied to derive the spectral function of finite nuclei and to calculate $n(k)$ in ^{16}O [29] was used as a basis to calculate $n(k)$ also in ^{40}Ca [30] and in

*Permanent address: Institute of Nuclear Research and Nuclear Energy, Bulgarian Academy of Sciences, Sofia 1784, Bulgaria.
†Institute of Nuclear Physics, NCSR "Demokritos," Aghia Paraskevi-Attiki, 15310 Greece.
‡Permanent address: Department of Theoretical Physics, University of Thessaloniki, GR-54006 Thessaloniki, Greece.

nuclei with $A=16$, 40, 48, 90, and 208 [31].

The model suggested in this work uses the transparency of the single-particle picture, being within the framework of a given correlation method by means of the natural orbital representation [33]. The latter enables us to specify in a natural way the high-momentum components in the momentum distribution which are of the same magnitude for various nuclear systems. The theoretical scheme of the method combines the mean-field predictions for the nucleon momentum distribution which are expected to be realistic at small k ($k\leqslant 2$ fm^{-1}) with the correlated part of the momentum distribution. In this sense, the method in this work has a similarity to that from [29] proposed for calculations of the spectral function $P(\mathbf{k},E)$, whose energy integral the nucleon momentum distribution is. We emphasize that in our work this is done upon the common ground of the natural orbital representation. The analyses of $n(k)$ performed in this work which use essentially the correlations contained in the ^{4}He nucleus (in contrast with the calculations based on nuclear matter results already mentioned) can diminish the theoretical uncertainties on $n(k)$ for medium-heavy nuclei.

II. THE MODEL

We start from the natural orbital representation [33], where the proton momentum distribution normalized to unity is of the form [2]

$$n(k)=\frac{1}{4\pi Z}\sum_{nlj}(2j+1)\lambda_{nlj}|\tilde{R}_{nlj}(k)|^2, \tag{1}$$

where λ_{nlj} is the natural occupation number for the state with quantum numbers (n,l,j) and

$$\sum_{nlj}(2j+1)\lambda_{nlj}=Z. \tag{2}$$

The radial part of the natural orbital in the momentum space $\tilde{R}_{nlj}(k)$ is related to the radial part of the natural orbital in the coordinate space $\tilde{R}_{nlj}(r)$ by

$$\tilde{R}_{nlj}(k)=(2/\pi)^{1/2}(-i)^l\int_0^\infty r^2 j_l(kr)\tilde{R}_{nlj}(r)dr, \tag{3}$$

where $j_l(kr)$ is the spherical Bessel function of order l. We call hole-state natural orbitals those natural orbitals for which the numbers λ_{nlj} are significantly larger than the remaining ones, called particle-state natural orbitals [34]. It was shown by the Jastrow correlation method [22] that the high-momentum components of the total $n(k)$ caused by short-range correlations are almost completely determined by the contributions of the particle-state natural orbitals. This fact, together with the approximate equality of the high-momentum tails of $n(k)$ for all nuclei with $A\geqslant 4$, allows us to make the main assumption of this work, namely, that the particle-state contributions to the momentum distribution are almost equal for all nuclei with $A\geqslant 4$.

Let us decompose the proton momentum distribution (1) into two terms:

$$n(k)=n_h(k)+n_p(k), \tag{4}$$

where the first term is the hole-state contribution

$$n_h(k)=\frac{1}{4\pi Z}\sum_{\alpha(nlj)}^{\alpha_F}(2j+1)\lambda_\alpha|\tilde{R}_\alpha(k)|^2, \tag{5}$$

while the second one is the particle-state contribution

$$n_p(k)=\frac{1}{4\pi Z}\sum_{\alpha_F}^{\infty}(2j+1)\lambda_\alpha|\tilde{R}_\alpha(k)|^2. \tag{6}$$

Using the assumed equality of the particle-state contributions $n_p(k)$ for all nuclei, we obtain the following general relation of the correlated proton momentum distribution of a nucleus (A,Z) with that of the ^{4}He nucleus:

$$n^{A,Z}(k)=N\left[n^{^4\mathrm{He}}(k)+\frac{1}{4\pi}\left(\frac{1}{Z}\sum_{nlj}^{F_{A,Z}}(2j+1)\lambda_{nlj}^{A,Z}|\tilde{R}_{nlj}^{A,Z}(k)|^2-\lambda_{1s_{1/2}}^{^4\mathrm{He}}|\tilde{R}_{1s_{1/2}}^{^4\mathrm{He}}(k)|^2\right)\right], \tag{7}$$

where

$$N=\left[1+\frac{1}{Z}\sum_{nlj}^{F_{A,Z}}(2j+1)\lambda_{nlj}^{A,Z}-\lambda_{1s_{1/2}}^{^4\mathrm{He}}\right]^{-1}, \tag{8}$$

and $F_{A,Z}$ is the Fermi level for the nucleus (A,Z).

Taking ^{40}Ca as an example the above expressions give

$$\begin{aligned}n^{^{40}\mathrm{Ca}}(k)=N\Bigg[&n^{^4\mathrm{He}}(k)+\frac{1}{4\pi}\Bigg(\frac{1}{10}\lambda_{1s_{1/2}}^{^{40}\mathrm{Ca}}|\tilde{R}_{1s_{1/2}}^{^{40}\mathrm{Ca}}(k)|^2+\frac{1}{5}\lambda_{1p_{3/2}}^{^{40}\mathrm{Ca}}|\tilde{R}_{1p_{3/2}}^{^{40}\mathrm{Ca}}(k)|^2+\frac{1}{10}\lambda_{1p_{1/2}}^{^{40}\mathrm{Ca}}|\tilde{R}_{1p_{1/2}}^{^{40}\mathrm{Ca}}(k)|^2\\&+\frac{3}{10}\lambda_{1d_{5/2}}^{^{40}\mathrm{Ca}}|\tilde{R}_{1d_{5/2}}^{^{40}\mathrm{Ca}}(k)|^2+\frac{1}{5}\lambda_{1d_{3/2}}^{^{40}\mathrm{Ca}}|\tilde{R}_{1d_{3/2}}^{^{40}\mathrm{Ca}}(k)|^2\\&+\frac{1}{10}\lambda_{2s_{1/2}}^{^{40}\mathrm{Ca}}|\tilde{R}_{2s_{1/2}}^{^{40}\mathrm{Ca}}(k)|^2-\lambda_{1s_{1/2}}^{^4\mathrm{He}}|\tilde{R}_{1s_{1/2}}^{^4\mathrm{He}}(k)|^2\Bigg)\Bigg]\end{aligned} \tag{9}$$

with

$$N=\left[1+\frac{1}{10}\lambda_{1s_{1/2}}^{^{40}\mathrm{Ca}}+\frac{1}{5}\lambda_{1p_{3/2}}^{^{40}\mathrm{Ca}}+\frac{1}{10}\lambda_{1p_{1/2}}^{^{40}\mathrm{Ca}}+\frac{3}{10}\lambda_{1d_{5/2}}^{^{40}\mathrm{Ca}}+\frac{1}{5}\lambda_{1d_{3/2}}^{^{40}\mathrm{Ca}}+\frac{1}{10}\lambda_{2s_{1/2}}^{^{40}\mathrm{Ca}}-\lambda_{1s_{1/2}}^{^4\mathrm{He}}\right]^{-1}. \tag{10}$$

As shown in [22], the hole-state natural orbitals are almost unaffected by the short-range correlations and, therefore, the functions $\tilde{R}_{nlj}(k)$ in Eq. (7) can be replaced by the corresponding Hartree-Fock single-particle wave functions

TABLE I. Experimental values of the proton momentum distribution in ^{4}He [26]. The normalization is $\int n(\mathbf{k})d^3\mathbf{k}=1$.

k (MeV/c)	$n(k)$ (fm^3)	k (MeV/c)	$n(k)$ (fm^3)
50	0.757 916	350	0.001 065
100	0.331 900	400	0.000 749
150	0.119 684	450	0.000 615
200	0.039 692	500	0.000 548
250	0.011 019	550	0.000 380
300	0.002 855		

or by the shell-model single-particle wave functions $R_{nlj}(k)$. The hole-state occupation numbers λ_{nlj} are close to unity within the Jastrow correlation method [22] and we can set them equal to unity with good approximation. The properties of the hole-state natural orbitals and occupation numbers and the decomposition of the proton momentum distribution in the hole- and particle-state contributions [Eqs. (4)–(6)] lead to a similarity of our model to that suggested for calculations of the spectral function in [29]. In it the mean-field predictions for the spectral function are combined with its correlated part extracted from the nuclear matter calculations and recalculated for finite nuclei within the local density approximation. In our model, the correlated proton momentum distributions can be calculated for any nucleus by means of the occupied shell-model wave functions and the proton momentum distribution of the ^{4}He nucleus which is taken from [26] and which contains short-range correlation effects.

III. CALCULATIONS AND DISCUSSION

In this work we calculate the proton momentum distribution for the nuclei ^{12}C, ^{16}O, ^{40}Ca, ^{56}Fe, and ^{208}Pb. Empirical estimations for $n(k)$ are available for the nuclei ^{12}C and ^{56}Fe [26].

In our calculations of proton momentum distributions we use two types of mean-field approximation (MFA) single-particle wave functions: (1) single-particle wave functions obtained within the Hartree-Fock method by using Skyrme effective forces and (2) multiharmonic oscillator single-particle (s.p.) wave functions (with different values of the oscillator parameter for each state) which lead to a simultaneous description of ground-state radii and binding energies [35,36]. In addition to [36], in our calculations the multiharmonic oscillator s.p. wave functions are orthonormalized. The values of all hole-state occupation probabilities λ_{nlj} in Eqs. (7) and (8) are set equal to unity. The empirical data of $n(k)$ for ^{4}He are taken from [26]. They are given in Table I. As mentioned in the Introduction, the extraction of the data for $n(k)$ is model dependent. Due to this, we give in Fig. 1 the comparison of the data for $n(k)$ in ^{4}He from [26] with the calculations within the variational Monte Carlo method from [19]. As can be seen from Fig. 1, the agreement is good and later we use in our calculations the data for $n(k)$ in ^{4}He from [26].

The calculated proton momentum distributions for the nuclei examined are given in Figs. 2–6, respectively. They are

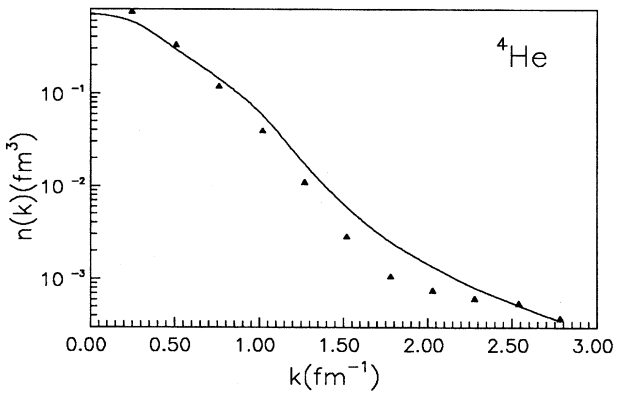

FIG. 1. Proton momentum distribution $n(k)$ versus k of ^{4}He. The solid triangles represent the data from [26]. The solid line is the result from [19]. The normalization is $\int n(\mathbf{k})d^3\mathbf{k}=1$.

compared with the available data for ^{12}C and ^{56}Fe from [26] and the proton momentum distributions obtained in various theoretical methods, namely, for ^{12}C from [22], for ^{16}O from [20,22,29–31], for ^{40}Ca from [22,30], and for ^{208}Pb from [31]. For the ^{12}C nucleus the results for the proton momentum distribution using the s.p. wave functions from the multiharmonic oscillator shell model but without including correlations are given in Fig. 7. Hence, the necessity of accounting for correlations becomes apparent.

We have the following purposes within the practical method suggested in this work for realistic calculations of the nucleon momentum distribution in light, medium, and heavy nuclei. (1) We wish to show that the high-momentum tail of the momentum distribution for any nucleus can be approximated by that for ^{4}He. We also check to what extent this approximation affects the central part of the momentum distribution. Since the low-momentum components of $n(k)$ are determined mainly by the hole-state natural orbitals con-

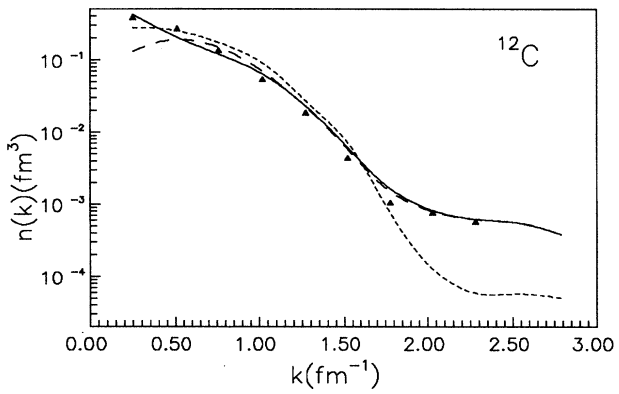

FIG. 2. Proton momentum distribution $n(k)$ versus k of ^{12}C. Calculations by using single-particle wave functions from the multiharmonic oscillator shell model [36] are presented by solid line and those by using Hartree-Fock single-particle wave functions by long-dashed line. The short-dashed line is $n(k)$ calculated in the Jastrow correlation method [22]. The solid triangles represent the data from [26]. The normalization is as in Fig. 1.

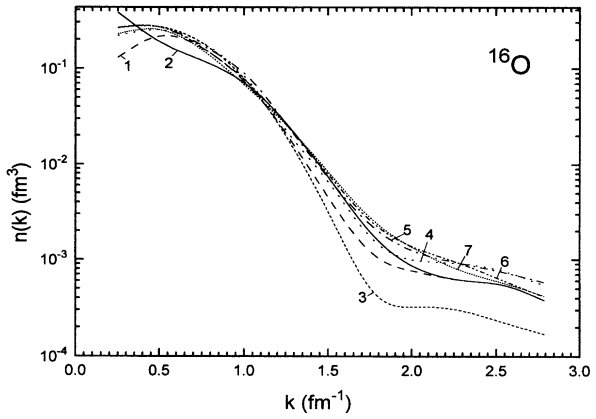

FIG. 3. Proton momentum distribution $n(k)$ versus k of ^{16}O. The lines 1 and 2 are the results of the present work using Hartree-Fock and multiharmonic oscillator shell model [36] single-particle wave functions, respectively. The lines 3, 4, 5, 6, and 7 are the results from [22,30,20,31,29], respectively. The normalization is as in Fig. 1.

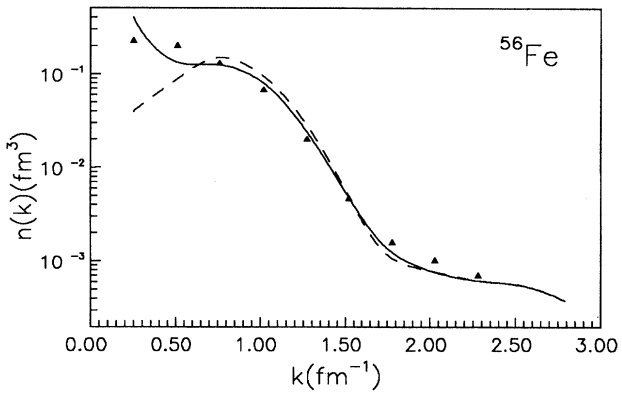

FIG. 5. Proton momentum distribution $n(k)$ versus k of ^{56}Fe. Calculations by using single-particle wave functions from the multiharmonic oscillator shell model [36] are presented by solid line and those by using Hartree-Fock single-particle wave functions by long-dashed line. The solid triangles represent the empirical data from [26]. The normalization is as in Fig. 1.

tribution, the justification of the use of shell-model or Hartree-Fock s.p. wave functions instead of hole-state natural orbitals can be checked. (2) We examine how well different s.p. shell-model wave functions can describe also the middle part of the momentum distribution which bridges the shell-model behavior of the central part and the non-shell-model behavior of the tail of the momentum distribution. (3) We wish to apply this method in which correlation effects are extracted from ^{4}He to calculate $n(k)$ as alternative to the methods in which correlations are extracted from nuclear matter and in this way, if possible, to diminish the theoretical uncertainties on the momentum distribution for medium-heavy nuclei.

One can see from Figs. 2 and 5 that the use of the single-particle wave functions from the multiharmonic oscillator shell model leads to better description of the experimental data for the central part of the momentum distribution than the use of the Hartree-Fock single-particle wave functions. In both cases the main deviations from the experimental data are for small momenta ($k \leq 0.5$ fm^{-1}). They are larger in the case when Hartree-Fock s.p. wave functions are used and this is a common feature of the results for all nuclei considered. This is due to the well-known fact [37] that the Hartree-Fock method cannot give a realistic wave function for the $1s$ state in the ^{4}He nucleus; namely, this function $[R^{^4\mathrm{He}}_{1s_{1/2}}(k)]$ takes part in the expression for $n(k)$ [Eq. (7)] in all nuclei. Both types of s.p. wave functions, however, give similar results for the middle part as well as for the tail of the momentum distribution in all cases considered.

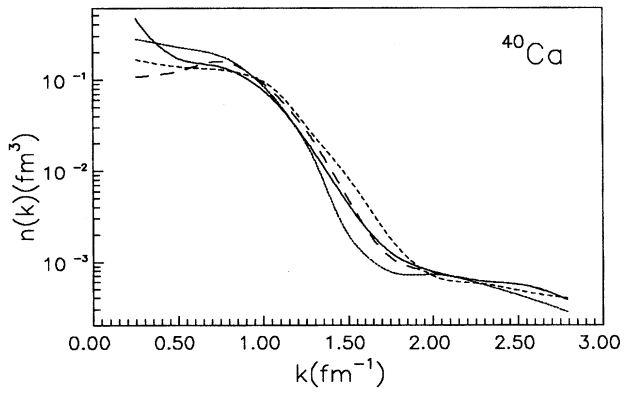

FIG. 4. Proton momentum distribution $n(k)$ versus k of ^{40}Ca. The solid and long-dashed lines are as in Fig. 2. The dotted line is $n(k)$ calculated in [22]. The short-dashed line is the result from [30]. The normalization is as in Fig. 1.

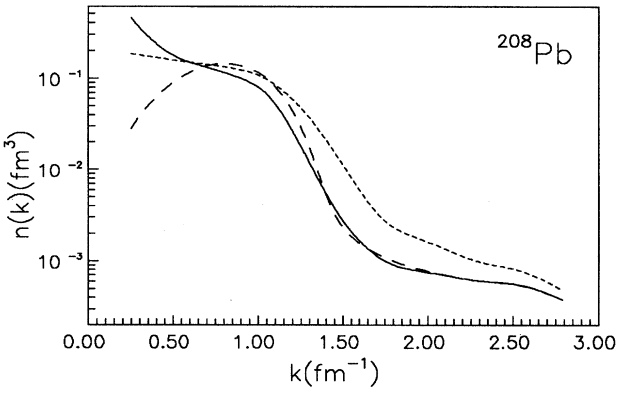

FIG. 6. Proton momentum distribution $n(k)$ versus k of ^{208}Pb. Calculations by using single-particle wave functions from the multiharmonic oscillator shell model [36] are presented by solid line and those by using Hartree-Fock single-particle wave functions by long-dashed line. The results from [31] are given by short-dashed line. The normalization is as in Fig. 1.

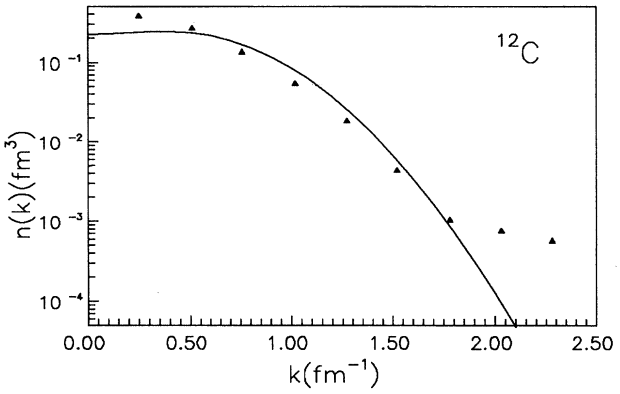

FIG. 7. Proton momentum distribution $n(k)$ versus k of ^{12}C. Calculations by using single-particle wave functions from the multiharmonic oscillator shell model [36] without including correlations are presented by solid line. The solid triangles represent the empirical data from [26]. The normalization is as in Fig. 1.

The comparison of the results obtained by using different mean-field single-particle wave functions can be useful for the proper choice of the latter in the applications of the model to practical calculations of $n(k)$ in cases when the knowledge of this quantity is necessary.

Our numerical check shows that the results obtained by using values of the occupation probabilities λ_{nlj} coming either from the experiments or from nucleon-nucleon correlation methods (e.g., the Jastrow one [22]) are almost the same as those obtained with $\lambda_{nlj}=1$. As long as the correlated values of λ_{nlj} do not differ significantly from the value $\lambda_{nlj}=1$, the improvement is not sizable.

We emphasize that only hole-state occupation probabilities and wave functions enter the main relationships of the model [Eqs. (7) and (8)]. In this way the suggested model can be easily applied to calculate momentum distributions in nuclei taking into account the nucleon-nucleon correlation effects. Concerning the particle-state contribution $n_p(k)$ [Eq. (6)] to the proton momentum distribution [which is accounted for in the model by means of the term $n^{^4\mathrm{He}}(k)$ in Eq. (7)] we would like to mention that the decisive role for the existence of the high-momentum components in $n_p(k)$ is the form of the particle-state natural orbitals $\tilde{R}_\alpha$ (which are strongly localized in coordinate space) but not the particle-state occupation numbers λ_α ($\alpha>\alpha_F$) [1,2,13,22].

As can be seen from Fig. 3 the results for the proton momentum distribution using the s.p. wave functions from the multiharmonic oscillator shell model are in agreement (at least for $k>0.8$ fm^{-1}) with those obtained in the variational Monte Carlo method [20] and in the calculations based on the local density approximation from [29–31]. The same can be seen from the comparison of our results for ^{40}Ca with those from [30] given in Fig. 4. In our opinion, the calculations within the suggested model (with correlation effects from ^{4}He) and the similarity of the results with those obtained in methods with correlations from nuclear matter can diminish in some sense the theoretical uncertainties on $n(k)$. We would mention that some differences remain between our results and those from [31] for ^{208}Pb in the middle part of the momentum distribution (Fig. 6).

It would be useful also to have estimations obtained extracting the correlation effects from nuclei lighter than ^{4}He, such as the deuteron or ^{3}He. As shown, however, in the variational correlation method (see Fig. 5 in [19]), the high-momentum components of $n(k)$ for the deuteron and ^{3}He, although with slopes similar to those of $n(k)$ for ^{4}He and nuclear matter, are quite different from them. At the same time, the high-momentum components of $n(k)$ for ^{4}He and nuclear matter are almost the same. This is the reason to use in our model correlation effects extracted from ^{4}He and to relate them to the properties of the nuclear interior.

IV. CONCLUSIONS

In the present paper a correlation model for calculating the proton momentum distribution in nuclei with $A>4$ is proposed. The model combines the mean-field part of the momentum distribution with its correlated part taken from ^{4}He on one and the same footing using the natural orbital representation. The estimation of the correlated part of $n(k)$ is based on the well-known fact that the high-momentum components of the momentum distribution normalized to unity (at $k\geq 2$ fm^{-1}) are nearly the same for all nuclei with $A\geq 4$. This fact, together with the use of the natural orbital representation, gives the possibility to obtain realistic momentum distributions in nuclei (including the regions of small momenta, $k<2$ fm^{-1}, and of intermediate momenta, $k\sim 2$ fm^{-1}) using only hole-state natural orbitals. The latter are replaced to a good approximation by shell-model single-particle wave functions. Thus the model gives a practical way for an easy calculation of the momentum distribution for any nucleus. The numerical results in this work confirm to a great extent the abilities of the suggested correlation model to give realistic estimations for the proton momentum distribution in ^{12}C and ^{56}Fe and to predict the behavior of $n(k)$ in ^{16}O, ^{40}Co, and ^{208}Pb nuclei. They are in agreement with the results for the proton momentum distribution in ^{16}O and ^{40}Co obtained within other theoretical methods in which the correlation effects are incorporated using nuclear matter results and with some empirical data for ^{12}C and ^{56}Fe obtained using the y-scaling method. The knowledge of the realistic proton momentum distributions obtained in this work would allow us to describe in a similar way as is done in [38] quantities which are directly measurable in processes of particle scattering by nuclei.

ACKNOWLEDGMENTS

Three of the authors (A.N.A., G.S.A., and S.E.M.) are grateful to the Nuclear Physics Laboratory of the University of Oxford for kind hospitality. The author A.N.A. is grateful to the Royal Society and the Bulgarian Academy of Sciences for support during his visit to the University of Oxford. The authors M.K.G., A.N.A., and M.V.S. would like to thank the Bulgarian National Science Foundation for partial financial support under Contracts No. Φ-32 and No. Φ-406. Finally, the authors G.S.A. and S.E.M. would like also to thank their home institutions for granting their sabbatical leaves.

[1] A. N. Antonov, P. E. Hodgson, and I. Zh. Petkov, *Nucleon Momentum and Density Distributions in Nuclei* (Clarendon Press, Oxford, 1988).
[2] A. N. Antonov, P. E. Hodgson, and I. Zh. Petkov, *Nucleon Correlations in Nuclei* (Springer-Verlag, Berlin, 1993).
[3] M. Jaminon, C. Mahaux, and H. Ngô, Phys. Lett. **158B**, 103 (1985).
[4] R. D. Amado, Phys. Rev. C **14**, 1264 (1976).
[5] J. G. Zabolitzky and W. Ey, Phys. Lett. **76B**, 527 (1978).
[6] A. N. Antonov, V. A. Nikolaev, and I. Zh. Petkov, Z. Phys. A **297**, 257 (1980).
[7] A. N. Antonov, I. S. Bonev, Chr. V. Christov, and I. Zh. Petkov, Nuovo Cimento A **100**, 779 (1988).
[8] F. Dellagiacoma, G. Orlandini, and M. Traini, Nucl. Phys. A **393**, 95 (1983).
[9] M. Traini and G. Orlandini, Z. Phys. A **321**, 479 (1985).
[10] O. Benhar, C. Ciofi degli Atti, S. Liuti, and G. Salmè, Phys. Lett. **177B**, 135 (1986).
[11] Y. Akaishi, Nucl. Phys. A **416**, 409c (1984).
[12] O. Bohigas and S. Stringari, Phys. Lett. **95B**, 9 (1980).
[13] A. N. Antonov, P. E. Hodgson, and I. Zh. Petkov, Nuovo Cimento A **97**, 117 (1987).
[14] M. Jaminon, C. Mahaux, and H. Hgô, Nucl. Phys. A **452**, 445 (1986).
[15] H. Morita, Y. Akaishi, and H. Tanaka, Prog. Theor. Phys. **79**, 863 (1988).
[16] S. Stringari, M. Traini, and O. Bohigas, Nucl. Phys. A **516**, 33 (1990).
[17] M. F. Flynn, J. W. Clark, R. M. Panoff, O. Bohigas, and S. Stringari, Nucl. Phys. A **427**, 253 (1984).
[18] S. Fantoni and V. R. Pandharipande, Nucl. Phys. A **427**, 473 (1984).
[19] R. Schiavilla, V. R. Pandharipande, and R. B. Wiringa, Nucl. Phys. A **449**, 219 (1986).
[20] S. C. Pieper, R. B. Wiringa, and V. R. Pandharipande, Phys. Rev. Lett. **64**, 364 (1990); Phys. Rev. C **46**, 1741 (1992).
[21] M. Baldo, I. Bombaci, G. Giansiracusa, U. Lombardo, C. Mahaux, and R. Sartor, Phys. Rev. C **41**, 1748 (1990).
[22] M. V. Stoitsov, A. N. Antonov, and S. S. Dimitrova, Phys. Rev. C **47**, R455 (1993); C **48**, 74 (1993); in *Proceedings of the 6th Workshop on Perspectives in Nuclear Physics at Intermediate Energies*, ICTP, Trieste, 1993 (World Scientific, Singapore, 1994), p. 236.
[23] A. N. Antonov, D. N. Kadrev, and P. E. Hodgson, Phys. Rev. C **50**, 164 (1994).
[24] D. B. Day, J. S. McCarthy, Z. E. Meziani, R. Minehart, R. Sealock, S. T. Thornton, J. Jourdan, I. Sick, B. W. Filippone, R. D. McKeown, R. G. Milner, D. H. Potterveld, and Z. Szalata, Phys. Rev. Lett. **59**, 427 (1987).
[25] C. Ciofi degli Atti, E. Pace, and G. Salmè, Nucl. Phys. A **497**, 361c (1989).
[26] C. Ciofi degli Atti, E. Pace, and G. Salmè, Phys. Rev. C **43**, 1155 (1991).
[27] X. Ji and R. D. McKeown, Phys. Lett. B **236**, 130 (1990).
[28] C. Ciofi degli Atti, E. Pace, and G. Salmè, Phys. Lett. **141B**, 14 (1984).
[29] O. Benhar, A. Fabrocini, S. Fantoni, and I. Sick, Nucl. Phys. A **579**, 493 (1994).
[30] G. Có, A. Fabrocini, and S. Fantoni, Nucl. Phys. A **568**, 73 (1994).
[31] D. Van Neck, A. E. L. Dieperink, and E. Moya de Guerra, Phys. Rev. C **51**, 1800 (1995).
[32] A. N. Antonov, M. V. Stoitsov, L. P. Marinova, M. E. Grypeos, K. N. Ypsilantis, and G. A. Lalazissis, Phys. Rev. C **50**, 1936 (1994).
[33] P.-O. Löwdin, Phys. Rev. **97**, 1474 (1955).
[34] D. S. Lewart, V. R. Pandharipande, and S. C. Pieper, Phys. Rev. B **37**, 4950 (1988).
[35] G. S. Anagnostatos, Int. J. Theor. Phys. **24**, 579 (1985).
[36] G. S. Anagnostatos, Can. J. Phys. **70**, 361 (1992).
[37] P. Ring and P. Schuck, *The Nuclear Many-Body Problem* (Springer-Verlag, New York, 1980).
[38] M. K. Gaidarov, A. N. Antonov, S. S. Dimitrova, and M. V. Stoitsov, Int. J. Mod. Phys. E **4** (4) (1995).